

STRUCTURE AND PROPERTIES OF ZnO THIN FILMS PREPARED BY REACTIVE ELECTRON BEAM EVAPORATION TECHNIQUE

M.E.L. Sabino¹; V.D. Falcão¹; C.P. Guerra¹; A.S. Diniz²; J.R.T. Branco^{1*}

¹ Fundação Centro Tecnológico de Minas Gerais, Laboratório de Engenharia e Modificações de Superfícies REDEMAT – Rede Temática em Engenharia de Materiais (CETEC, UFOP, UEMG)

Av. José Cândido da Silveira, 2000 – Horto, 31170-000, Belo Horizonte, MG, Brasil

² Companhia Energética de Minas Gerais – CEMIG

Received: December 6, 2006; Revised: March 12, 2007

Key words: thin films, ZnO, electron beam evaporation

ABSTRACT

Zinc oxide has been used as transparent and conducting oxide film in solar cells and electrochromic devices. In this work, ZnO thin films have been deposited by reactive electron beam evaporation technique with argon-oxygen plasma assistance. The films have been deposited on glass substrate. After the deposition, the films were annealed at 550°C during 2 hours in an oxidant atmosphere to improve its optical and electrical properties. The films were characterized by atomic force microscopy, UV/VIS/NIR spectroscopy, electrical resistivity and X-ray diffraction. The films are adherent and present high roughness, low transmittance and low crystallinity. After the thermo-chemical treatment there was an increase in optical transmittance, in crystallinity and a decrease of the absorption coefficient in the visible spectral region and of the electrical resistivity. Furthermore, the results of atomic force microscopy and DRX indicate that this treatment promotes a significant change of the surface texture and of the grain size.

1. INTRODUCTION

Transparent conductive oxides (TCO) are valuable front electrode for various thin film solar cells. The materials used as TCO films are wide band gap semi conductors with low specific resistance and high transparency in the visible and near infrared wavelength range. Because of their chemical stability, good electro-optical properties, large band gap ($E_g = 3.4$ eV, direct), abundance in nature and low toxicity, the ZnO thin films have emerged as one of the most used transparent conductive oxides [1]. Furthermore because of its transparency for wavelengths between 380nm-900nm, ZnO is an interesting material for application in integrated optical devices [2].

Thin films of zinc oxide have been used as the transparent conducting film in SHJ (silicon heterojunction), as in the HIT cells (Heterojunction with Intrinsic Thin Layer) solar cells which are deposited on amorphous hydrogenated silicon film. ZnO films have been deposited by several deposition techniques such as laser ablation [3], spray pyrolysis

[4], sputtering [5,6], electron beam evaporation [7,8] and metal-organic chemical vapor [9] on a variety of substrates. In this work ZnO films was deposited on glass substrates by reactive electron beam evaporation. Structural and optical properties of ZnO films in as-deposited and annealed condition are evaluated. The influence of annealing on the properties of the ZnO films discussed. Optical and electrical properties and morphology have been measured in order to rationalize the effect of the annealing process.

2. EXPERIMENTAL

The ZnO thin films were deposited by reactive electron beam evaporation technique over glass substrate. A schematic of deposition chamber is shown in Figure 1. A zinc target with high-purity (99.99%) was used as ZnO source. The films have been deposited with argon-oxygen plasma assistance, at 3.2×10^{-3} mBar. The substrate to target distance was 27 cm and the beam power was 3200 W. The substrate temperature was 230°C and the deposition time was 25 min. After deposition, the films were annealed in O₂ atmosphere at 550°C for 2 hours.

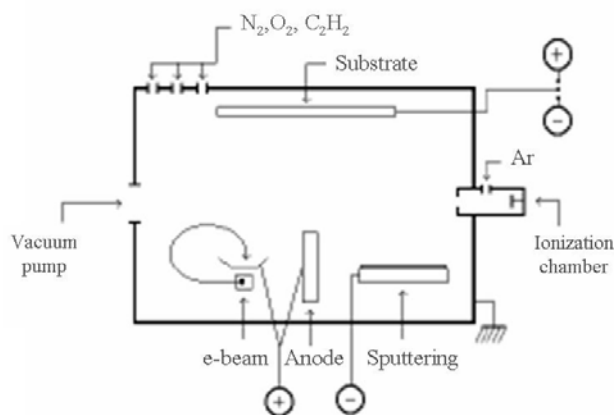


Figure 1 - Scheme of deposition chamber.

* jose.branco@cetec.br

The structural properties of the films were studied using X-ray diffractometry with a sample rotating device and Cu K α radiation. The thicknesses were measured using a Dektak profilometer. Optical measurements were carried out using a spectrophotometer from N & K Technologies, model Analysis 1280. The optical measurements were performed taking glass as reference. From these data, and using the Swane-poel's method, which is based on Manificier's idea [1], the thickness and the refraction index n were calculated. The surfaces of the films were analyzed by Atomic Force Microscopy (AFM Dimension 3100 Digital Instrument) and the electrical resistivity was measured by the four-probe technique.

3. RESULTS AND DISCUSSION

Figure 2 shows X-ray diffraction spectrum of the thin films. An increase in the film crystallinity after the annealing is observed.

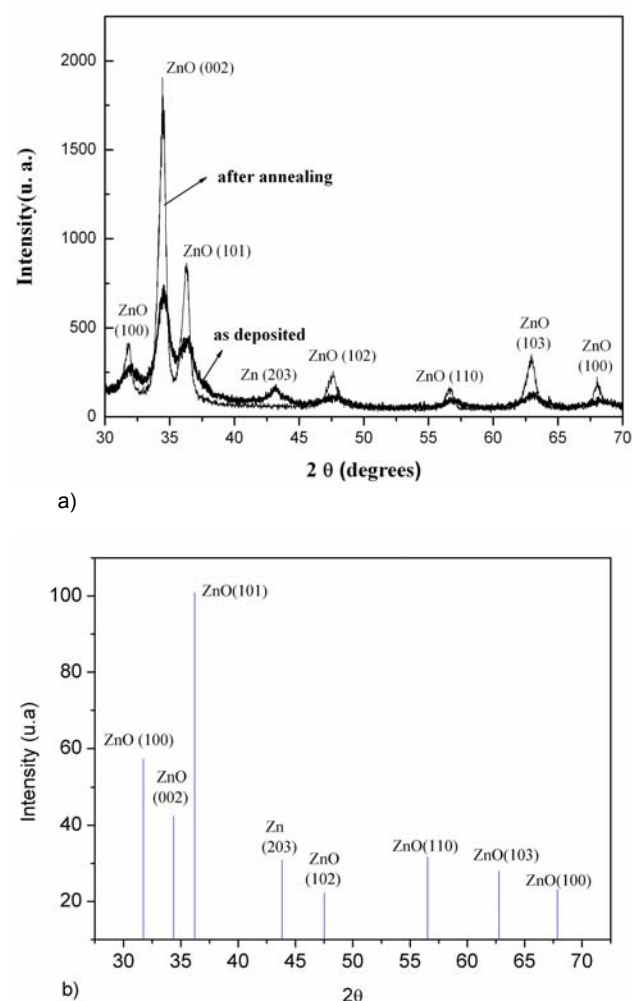


Figure 2 - X-ray diffraction patterns of ZnO films. a) as deposited and after annealing, b) standard JC PDS.

The ZnO diffraction peaks at (100), (002), (101), (102), (110), (103) and (100), crystal orientation are clearly identified, Fig. 2.a, centered at 31.76°, 34.5°, 36.21°, 47.51°, 56.59°, 62.83° and 67.97°, respectively. A Zn peak at (203), centered at 43.68°, also identified. The Zn peak disappears after annealing treatment, Figure 2-b. The average grain size of ZnO nanoparticles, t , can be estimated by the Scherrer's equation:

$$t = \frac{k\lambda}{B \cos \theta} \quad (1)$$

where k is a constant, about 1, generally considered as 0,9; λ the wavelength of Cu K α radiation, 1.5405 Å, and B is the full-width at half-maximum (FWHM). The sample was continuously rotated during the diffraction measurement. The diffraction intensity was measured as a function of diffraction angle. The Table A show the peaks orientation and the grain size of as deposited and treated films. The intensity of the (002) peak increased likely due to the increase of the films crystallinity.

Table A - Grain size of as deposited and treated films, as calculated from different X ray diffractions peaks.

Peak hkl	Grain size	
	as deposited	after annealing treatment
(002)	6,74nm	13,27nm
(101)	4,6nm	12,64nm

The AFM images of films as deposited (a) and after heat treated (b) are shown in Figure 3. The crystallites are separated by pinholes and there are inhomogeneities at the two surfaces. The annealing led to changes of the surface texture and of the grain size. The latter is larger after annealing treatment than it is as deposited, as confirmed by XRD measurements. Moreover, it was observed that the post-treatment led to change in the average roughness, from 27.08 nm to 24.14 nm for the as deposited and treated films, respectively.

Figure 4 shows the wavelength dependence of optical transmittance spectra of the ZnO thin films deposited on glass. The films show good adherence but poor transmittance, about 6 % in the visible region. After annealing the films became more transparent and shown standard fringes. The thermo-chemical treatment increases the transmittance to 91% in the visible region. This improvement is likely due to the reestablishment of the stoichiometry of ZnO through the incorporation of oxygen. The thickness of annealed films measured by profilometry increases from 0.65 μm to 1 μm . This increase of thickness is probably due to the formation of oxides in the film surface.

The transmittance data were treated according to Swane-poel's method, which is based on Manificier's idea. The envelopes curves of interference maximum and minimum are created, as shown in the Figure 5.

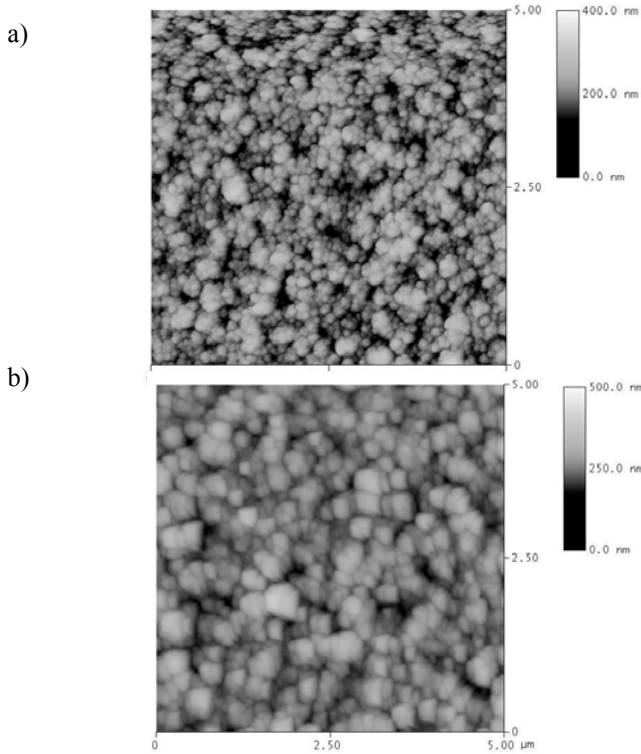


Figure 3 – AFM images of ZnO films (a) as deposited and (b) after annealing in oxidant atmosphere.

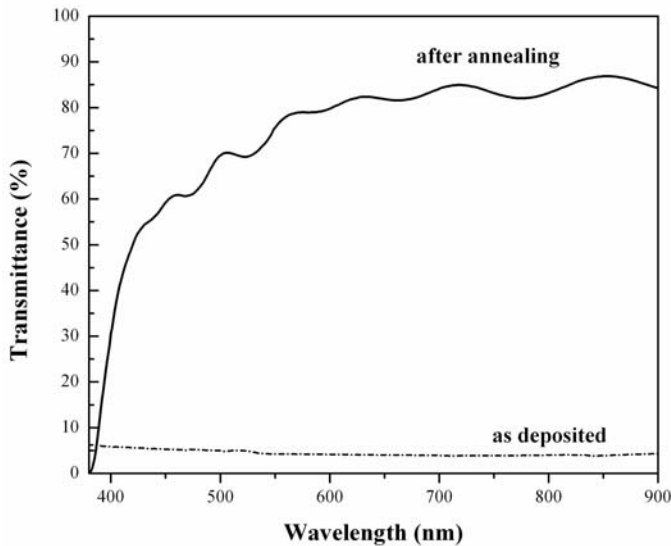


Figure 4 – Transmittance spectra of e-beam evaporated ZnO films on glass as deposited (dashed line) and after annealing (solid line).

First, the approximate value of the refractive index of the film n_1 in the spectral region of medium and weak absorption, can be calculated by the expression:

$$n = \left[N_1 + (N^2 - n_0^2 - n_1^2)^{1/2} \right]^{1/2} \quad (2)$$

where:

$$N = \frac{(n_0 - n_1^2)}{2} + 2n_0n_1 \left[\frac{T_{\max} - T_{\min}}{T_{\max} T_{\min}} \right] \quad (3)$$

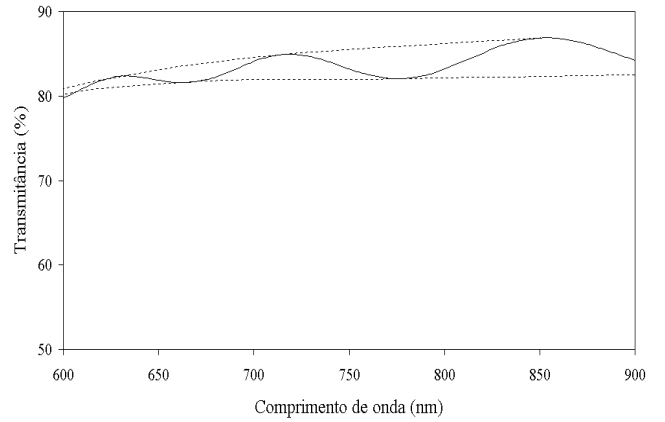


Figure 5 - Transmittance spectra of e-beam evaporated ZnO films on glass after annealing with envelope hatched curves.

The glass and air refractive index used were $n_0 = 1$ and $n_1 = 1.51$, respectively; T_{\max} and T_{\min} are the transmission maximum and the corresponding minimum at a certain wavelength λ . Alternatively, one of these values is an experimental interference extreme and the other one is derived from the corresponding envelope curve. The film thickness can be calculated from the refractive index corresponding to adjacent extreme values ($n(\lambda_1) - n(\lambda_2)$) through the following expression [11]:

$$t = \frac{M(\lambda_1 - \lambda_2)}{2[\lambda_1 n(\lambda_2) - \lambda_2 n(\lambda_1)]} \quad (4)$$

with $M=1$ for two adjacent extremes of the same type (maximum-maximum or minimum-minimum) and $M=1/2$ for two adjacent unlike extremes (maximum-minimum or minimum maximum).

The absorption index (K) is determined from the following relation:

$$K = -\ln \left\{ \frac{\left[C_1 \left[1 - \left(\frac{T_{\max}}{T_{\min}} \right)^{1/2} \right] \right]}{\left[C_2 \left[1 + \left(\frac{T_{\max}}{T_{\min}} \right)^{1/2} \right] \right]} \right\} t^{-1} \quad (5)$$

where

$$C_1 = (n + n_0)(n_1 + n) \quad (6)$$

$$C_2 = (n - n_0)(n_1 - n) \quad (7)$$

The calculated refractive index (n), thickness (t) and absorption index (K) are listed in Table B.

Table B – Calculated thickness (t), refractive index (n) and absorption index (K) for ZnO films deposited on glass, after annealing.

n	1,66
$t(\text{nm})$	780
$K(\text{cm}^{-1})$	$2,07 \cdot 10^{-4}$

These values are near to values found in literature [11]. The Table C show the resistivity values of the films as deposited and after annealing.

Table C – Values of electrical resistivity for ZnO films deposited on glass, before and after annealing.

ZnO thin film	ρ ($\Omega \cdot \text{cm}$)
as deposited	$8,711 \times 10^2$
after annealing	$5,31 \times 10^1$

There was a decrease of electrical resistivity after annealing. This decrease in the electrical resistivity probably due to the film oxidation and grain growth as shown by AFM and X ray diffraction results and possibly recrystallization [12].

4. CONCLUSIONS

Zinc oxide thin films were deposited by reactive electron beam evaporation technique with argon-oxygen plasma assistance. The annealing in oxidant atmosphere improves the optical and electrical properties of ZnO films. The AFM analyses show that the as deposited films have grain size smaller than treated films and that annealing promoted a homogenization and likely recrystallization and or grain growth of ZnO. The indirect Swanepoel's method allowed calculating the thickness and the optical constants of the film from the transmission spectrum.

ACKNOWLEDGEMENTS

This work was supported by CAPES, FAPEMIG and CEMIG. The authors are thankful to Votorantin Metals; Dr^a Margareth Spangler Araújo, Dr. José Mário Carneiro Villela and Vitor P. Gouveia, from Fundação Centro Tecnológico de Minas Gerais.

REFERENCES

1. PEARTON, S.J.; NORTON, D.P.; IP, K.; HEO, Y.W.; STEINER, T., *Progress in Materials Science* 50 (2005) 293–340.
2. HEIDEMAN, R.G.; LAMBECK, P.V.; GARDENIERS J.G.E., *Optical Materials* 4 (1995) 741-755.
3. HENLEY, S.J.; ASHFOLD, M.N.R.; CHERNS, D. *Surface and Coatings Technology* 177–178 (2004) 271–276.
4. BOUGRINE, A.; EL HICHO, A.; ADDOU, M.; EBOU, J.; KACHOUANE, A.; TROYON, M., *Materials Chemistry and Physics* 80 (2003) 438–445.
5. ONDO-NDONG, R.; FERBLANTIER, G.; PASCAL-DELANNOY, F.; FOUCHARAN, A., *Microelectronics Journal* 34 (2003) 1087–1092.
6. ONDO-NDONG, R.; PASCAL-DELANNOY, F.; BOYER, A.; GIANI, A.; FOUCHARAN, A., *Materials Science and Engineering B* 97 (2003) 68–73.
7. WU, H.Z.; HE, K.M.; QIU, D.J.; HUANG, D.M., *Journal of Crystal Growth* 217 (2000) 131–137.
8. AGHAMALYAN, N.R.; GAMBARYAN, I.A.; GOULANIAN, E.K.; HOVSEPYAN, R.K.; KOSTANYAN, R.B.; PETROSYAN, S.I.; VARDANYAN, E.S.; ZERROUK, A.F., *Semiconductor Science and Technology* 18 (2003) 525–529.
9. YOUN, C.J.; JEONG, T.S.; HAN, M.S.; KIM, J.H., *Journal of Crystal Growth* 261 (2004) 526–532.
10. MADELUNG, O., *Semiconductors Basic Data*. 2ed. Tokyo: Springer, 1996.
11. SANCHEZ-GONZALEZ, J.; DIAZ-PARRALEJO, J.A.; ORTIZ A.L.; GUIBERTEAU, F., *Applied Surface Science* (2005) 6013-6017.
12. AL ASMAR, R.; FERBLANTIER, G.; MAILLY, F.; GALL-BORRUT P.; FOUCHARAN, A., *Applied Surface Science* 245 (2005) 384–390.